

000 COUNTERFACTUAL PREDICTION WITH CROSS- 001 002 WORLD DEPENDENCE 003 004

005 **Anonymous authors**

006 Paper under double-blind review

007 008 ABSTRACT 009 010

011 We study the problem of estimating the expected retrospective counterfactual out-
012 come for an individual with covariates x and observed outcome y , defined as
013 $\mu(x, y) = \mathbb{E}[Y(1) \mid X = x, Y(0) = y]$, and constructing valid prediction in-
014 tervals under the Neyman–Rubin superpopulation model with i.i.d. units. This
015 quantity is generally unidentified without additional assumptions. To link the ob-
016 served and unobserved potential outcomes, we work with a cross-world corre-
017 lation function $\rho(x) = \text{cor}(Y(1), Y(0) \mid X = x)$ that quantifies their dependence
018 given the covariates. Plausible bounds on $\rho(x)$, often informed by domain knowl-
019 edge, enable a principled approach to this otherwise unidentified problem. Given
020 ρ , we develop an estimator $\hat{\mu}_\rho(x, y)$ and prediction intervals $C_\rho(x, y)$ that sat-
021 isfy $P[Y(1) \in C_\rho(X, Y(0))] \geq 1 - \alpha$ under standard causal assumptions and
022 Gaussian dependence structure. Almost all existing methods correspond to ei-
023 ther the case $\rho = 0$ (ignoring the factual outcome), or $\rho = 1$ (constant treatment
024 effects). We show that interpolating between these cases via cross-world depen-
025 dence yields estimators that are theoretically optimal under (asymptotic) Gaussian
026 assumptions. In practice, this leads to substantial empirical improvements across
027 a wide range of scenarios.

028 1 INTRODUCTION 029

030 At its core, causal inference pursues two goals: assessing what would have happened to an individ-
031 ual under an alternative treatment, and predicting how a new individual will benefit from treatment
032 (Rubin, 2005). For answering the second goal, the literature focuses on average treatment effects
033 (ATE) or conditional average treatment effects (CATE). However, estimating retrospective counter-
034 factuals (first goal) is often more challenging, as it requires untestable assumptions, connected to
035 the Pearl’s third ladder of causation (Pearl & Mackenzie, 2019). Estimates of counterfactuals are
036 critical in many fields: in medicine, they enable evaluating how a patient might have responded to a
037 different treatment (Imbens & Rubin, 2015); in criminal law, they underpin the “but-for” test of cau-
038 sation, which assesses liability based on whether harm would have occurred absent the defendant’s
039 action (Wright, 1985).

040 Consider a medical scenario in which a patient, James, arrives at a hospital with covariates $X = x$
041 (e.g., age, weight, and other characteristics), does not receive the treatment ($T = 0$), and experiences
042 an outcome $Y(0) \in \mathbb{R}$. Estimating his retrospective counterfactual outcome $Y(1)$ is central to
043 causal reasoning. In high-stakes settings such as healthcare, it is equally important to quantify the
044 uncertainty in individual treatment effects (ITEs); that is, to construct a set $C \subseteq \mathbb{R}$ that contains
045 $Y(1)$ with high probability.

046 Existing methods primarily focus on estimating the CATE, defined as $\tau(x) = \mu_1(x) - \mu_0(x)$,
047 where $\mu_t(x) = \mathbb{E}[Y(t) \mid X = x]$ for $t = 0, 1$ can be estimated via e.g. random forest (Wager
048 & Athey, 2018). The missing counterfactual is often imputed either by $\hat{Y}(1) = Y(0) + \hat{\tau}(X)$, by
049 $\hat{Y}(1) = \hat{\mu}_1(X)$, or through a matching-based approach. Some notable exceptions are presented in
050 Section 2 and Appendix A.1.

052 Many existing approaches condition only on covariates X , overlooking the observed (factual) out-
053 come $Y(0)$, which often contains valuable individual-specific information. For instance, if James
left the hospital healthy after not receiving treatment ($T = 0$), it is highly likely that he would also

054 be healthy under the counterfactual scenario in which he received treatment ($T = 1$). Incorporating
 055 the factual outcome alongside the covariates can therefore refine individual-level predictions and
 056 improve the accuracy of estimated counterfactuals.

057 In this work, we propose leveraging covariates *and* the factual outcome to enhance counterfactual
 058 prediction. Specifically, instead of estimating $\mathbb{E}[Y(1) | X = x]$, we aim to construct point estimates
 059

$$060 \hat{\mu}_\rho(x, y) \quad \text{for} \quad \mathbb{E}[Y(1) | X = x, Y(0) = y], \quad (1)$$

062 and $(1 - \alpha)$ -level prediction intervals $C_\rho(x, y)$ for the counterfactuals satisfying:

$$064 P(Y(1) \in C_\rho(x, y) | X = x, Y(0) = y) \geq 1 - \alpha, \quad (2)$$

065 for $\alpha \in (0, 1)$ (typically $\alpha = 0.1$). Conditioning on the factual outcome introduces a fundamental
 066 challenge: since both potential outcomes are never observed for the same individual, the joint dis-
 067 tribution of $(Y(0), Y(1))$ is unidentifiable without further assumptions. To address this, we adopt a
 068 class of assumptions known as cross-world assumptions.

069 **Definition 1** (Bodik et al. (2025)). *In the Neyman–Rubin super-population model with i.i.d. units,
 070 the dependence structure (conditional correlation) between the potential outcomes $Y(1), Y(0)$, con-
 071 ditioned on the observed covariates X , is defined as:*

$$073 \rho(x) = \text{cor}(Y(1), Y(0) | X = x).$$

075 We refer to an assumption about ρ as *cross-world assumption*.

076 The term “cross-world assumption” was first introduced in Bodik et al. (2025), and related ideas
 077 have appeared in prior literature (see Section 2), often represented via an additive structural equation
 078 model:

$$080 Y(0) = \mu_0(X) + \varepsilon_0, \quad Y(1) = \mu_1(X) + \varepsilon_1, \quad \text{where } \text{cor}(\varepsilon_1, \varepsilon_0) = \rho(X).$$

082 Although ρ is not identifiable from data, postulating plausible values or bounds from domain experts
 083 is often both feasible and well-aligned with how humans make judgments. Observing one potential
 084 outcome often conveys information about the other, beyond what is captured by covariates.

086 **Our contributions.** Given a specified value (or a set of plausible values) of ρ , we propose a con-
 087 sistent counterfactual point estimator equation 1 and valid prediction intervals equation 2, under
 088 standard causal assumptions and Gaussian copula. For clarity, we focus on the case $T = 0$ and
 089 the counterfactual outcome is $Y(1)$; the reverse case is analogous. While the formal definitions of
 090 $\hat{\mu}_\rho(x, y)$ and $C_\rho(x, y)$ are given in Section 3, we present here the key property that motivates their
 091 construction:

092 **Theorem 1** (Motivation and optimality). *Let $x \in \mathcal{X}$ and $\rho(x) = \text{cor}(Y(0), Y(1) | X = x) \in$
 093 $[-1, 1]$. Assume an asymptotic scenario: $\hat{\mu}_t(x) = \mu_t(x)$ and suppose that we found conditionally
 094 valid prediction intervals:*

$$095 \mathbb{P}(Y(t) \leq \hat{\mu}_t(x) + u_t(x) | X = x) = 0.95, \quad \mathbb{P}(Y(t) \geq \hat{\mu}_t(x) - l_t(x) | X = x) = 0.95, \quad t = 0, 1.$$

097 If $(Y(1), Y(0)) | X = x$ is Gaussian, then C_ρ prediction intervals, defined in Section 3, are optimal
 098 in a sense that it is the smallest set satisfying:

$$100 \mathbb{P}(Y(1) \in C_\rho(X, Y(0)) | X = x, Y(0) = y) \geq 0.9.$$

102 Moreover, $\hat{\mu}_\rho(x, y)$ is the optimal point predictor in the sense that it minimizes the mean squared
 103 error:

$$104 \hat{\mu}_\rho(x, y) = \underset{c \in \mathbb{R}}{\text{argmin}} \mathbb{E}[(Y(1) - c)^2 | X = x, Y(0) = y].$$

106 Our proposed C_ρ intervals are introduced in Section 3, following preliminaries in Section 2. In
 107 Section 4, we discuss empirical evaluation compared to other methods. Section 5 concludes.

108 **2 PRELIMINARIES, RELATED WORK AND CROSS-WORLD ASSUMPTION**
109110
111 We adopt the Neyman-Rubin potential outcomes framework (Rubin, 2005), where each unit i has
112 potential outcomes $Y_i(1)$ and $Y_i(0)$, covariates $X_i \in \mathcal{X} \subseteq \mathbb{R}^d$, and treatment assignment $T_i \in$
113 $\{0, 1\}$. The observed outcome is $Y_i = T_i Y_i(1) + (1 - T_i) Y_i(0) \in \mathcal{Y} \subseteq \mathbb{R}$, while the $ITE_i =$
114 $Y_i(1) - Y_i(0)$ remains unobservable. We assume $(Y_i(1), Y_i(0), T_i, X_i) \stackrel{i.i.d.}{\sim} (Y(1), Y(0), T, X)$, for
115 a generic random vector $(Y(1), Y(0), T, X)$. The conditional average treatment effect (CATE) is
116 defined as $\tau(x) = \mu_1(x) - \mu_0(x)$ with $\mu_t(x) = \mathbb{E}[Y(t) | X = x]$.117 We impose **strong ignorability** and **overlap**, meaning $(Y(1), Y(0)) \perp\!\!\!\perp T | X$ and $0 < \pi(x) < 1$
118 for all $x \in \mathcal{X}$, where $\pi(x) = \mathbb{P}(T = 1 | X = x)$ denotes the propensity score. These conditions en-
119 sure that treatment is as-if randomly assigned given covariates and that both treatments are feasible.
120 Under these assumptions, CATE is identified via $\mu_t(x) = \mathbb{E}[Y | T = t, X = x]$ (Wager, 2024).121 We note that some authors use the terms “ITE” and “CATE” interchangeably, which can lead to
122 confusion. Here, ITE is a latent, unit-specific quantity, while the CATE is an unknown function,
123 defined as the conditional expectation of the ITE given covariates.
124125 **2.1 RELATED WORK: CROSS-WORLD ASSUMPTION**
126127
128 In the potential outcomes framework, the joint distribution of $(Y(1), Y(0)) | X$ is unidentifiable
129 because only one potential outcome is observed per unit. While CATE can be identified without
130 assumptions on this joint law, quantities such as variance, quantiles, or prediction intervals of ITE
131 generally depend on the cross-world correlation $\rho(X) = \text{cor}(Y(1), Y(0) | X)$ (Rubin, 1990; Ding
132 et al., 2019). This has been studied in joint distribution modeling (Heckman et al., 1997; Fan &
133 Park, 2010), quantile treatment effect estimation (Firpo, 2007) and nonparametric bounds using
134 copulas (Zhang & Richardson, 2025a; b; Nelsen et al., 2001). Andrews & Didelez (2021) highlight
135 the implausibility of cross-world independence assumptions in mediation analysis; we complement
136 these by parameterizing cross-world dependence via $\rho(x)$.137 Bodik et al. (2025) and Cai et al. (2022) argue that in many real-world applications ρ is almost always
138 non-negative and often substantially positive due to shared latent factors affecting both potential
139 outcomes. Formally, consider a model where $Y(1) = \mu_1(X) + H + \tilde{\varepsilon}_1$ and $Y(0) = \mu_0(X) + H + \tilde{\varepsilon}_0$,
140 where $X \in \mathbb{R}^d$ are observed covariates, $H \perp\!\!\!\perp (X, T)$ is an unobserved factor influencing both
141 potential outcomes, and $\tilde{\varepsilon}_0 \perp\!\!\!\perp \tilde{\varepsilon}_1$ are idiosyncratic noise terms. Conditioning on X , it is easy
142 to derive that $\rho(X) = \text{cor}(Y(1), Y(0) | X) = \frac{\text{var}(H)}{\sqrt{\text{var}(\tilde{\varepsilon}_0) \text{var}(\tilde{\varepsilon}_1)}} \geq 0$. Whenever $\text{var}(H) > 0$,
143 the shared influence of H induces strictly positive correlation between $Y(1)$ and $Y(0)$, even after
144 adjusting for X . Moreover, if the treatment has no or very small effect, then $Y(1) \approx Y(0)$ and
145 hence $\rho \approx 1$.146 Following Bodik et al. (2025), the choice of $\rho(x)$ can be guided by practitioners by asking: “What
147 proportion of the outcome variability is driven by latent factors that influence both potential out-
148 comes in a similar way?” In other words, what values are plausible for $\frac{\text{var}(\text{shared latent effects})}{\text{var}(\text{idiosyncratic noise})}$. In many
149 complex systems, it is reasonable to expect a substantial contribution from shared latent compo-
150 nents, suggesting that $\rho(x)$ may typically exceed 0.5. At the same time, $\rho(x)$ is rarely close to 1,
151 since treatment effects generally exhibit heterogeneity even among individuals with the same ob-
152 served covariates X . This is not a universal rule, but a practical guideline grounded in the idea how
153 latent common causes in many real-world systems influence both $Y(0)$ and $Y(1)$.154 As an example, consider a clinical trial testing a new drug for reducing blood pressure, where the
155 treatment is randomly assigned and standard causal assumptions hold. Let $Y_i(1)$ denote patient i ’s
156 blood pressure after receiving the drug and $Y_i(0)$ after receiving a placebo. Even though baseline
157 covariates such as age, weight, and existing conditions are observed, unmeasured factors like genetic
158 predisposition can strongly influence both potential outcomes. A patient with naturally resilient car-
159 diovascular health will likely exhibit relatively low blood pressure regardless of treatment, whereas
160 a patient with severe underlying issues will tend to have higher readings in both scenarios. These
161 persistent latent traits induce a positive dependence between $Y_i(1)$ and $Y_i(0)$ even after adjusting
for observed covariates. Given this medical knowledge, it is reasonable to assume $\rho(x)$ is not only

positive but possibly large, likely above 0.5. See Bodik et al. (2025) for more examples when some domain knowledge about ρ is available.

2.2 RELATED WORK: RETROSPECTIVE COUNTERFACTUALS FOR IN-STUDY UNITS

Inferring individual counterfactual outcomes is fundamentally a missing data problem (Ding & Li, 2018). Many methods for counterfactual prediction use CATE-adjusted imputation $\hat{Y}_i(1) = Y_i(0) + \hat{\tau}(X_i)$, where $\hat{\tau}$ is estimated using doubly-robust estimator, random forests or S/T-learner (Wager, 2024; Künnel et al., 2019; Athey et al., 2019). Other approaches directly model the treated outcome as $\hat{Y}_i(1) = \hat{\mu}_1(X_i)$, thereby ignoring information contained in the observed outcome $Y_i(0)$ (possibly using control group only for the propensity estimation, Lei & Candès (2021)).

Classic counterfactual prediction methods target $\mathbb{E}[Y(T) | X]$ without conditioning on $Y(0)$. For instance, Kim et al. (2022) propose a doubly robust estimator for counterfactual classification that directly models the treated outcome distribution, and McClean et al. (2024) develop nonparametric estimators for conditional incremental effects (based on stochastic propensity interventions) with a similar goal of directly estimating $\mathbb{E}[Y(1) | X]$. More recently, Kim (2025) introduces a semi-parametric counterfactual regression framework that likewise estimates $\mathbb{E}[Y(1) | X]$ using flexible machine learning. These approaches forego individual-level imputation using $Y(0)$, instead relying on robust modeling of the treated outcome. Most existing methods focus on minimizing the Precision in Estimation of Heterogeneous Effects (PEHE), defined as $\mathbb{E}_X (\hat{\tau}(X) - \tau(X))^2$, which targets CATE recovery. However, optimizing PEHE is not well suited for inference about counterfactuals.

There are a few notable exceptions where the construction of $\hat{Y}_i(1)$ follows a different principle. **Adversarial approaches:** Yoon et al. (2018) introduce GANITE, which employs adversarial training to generate $\hat{Y}_i(1)$. Although GANITE innovatively bypasses strict model assumptions, it focuses on PEHE and relies on black-box adversarial neural networks without explicitly modeling the joint distribution of potential outcomes. It typically performs well with large dimensions but poorly with small ones. **Bayesian causal inference:** Missing counterfactuals are treated as latent variables, and uncertainty is integrated through the posterior distribution. For example, Alaa & van der Schaar (2017) propose a Bayesian multitask Gaussian process to jointly model $(Y(1), Y(0)) | X$, producing posterior distributions over the potential outcomes. While Bayesian methods offer coherent uncertainty quantification, they rely on strong modeling assumptions and can be sensitive to prior specifications (Li et al., 2022). Moreover, they can be restrictive when aiming to leverage flexible modern machine learning techniques. **Matching methods:** Matching-based approaches (Hur & Liang, 2024) estimate counterfactual outcomes by pairing individuals i, j with similar covariates but different treatments, and approximating the ITE as $Y_j(1) - Y_i(0)$. However, this construction implicitly assumes independence between the potential outcomes ($\rho = 0$). To our knowledge, existing matching methods do not incorporate matching mechanisms that depend directly on the value of Y_i .

More detailed literature review can be found in Appendix A.1.

3 CONSTRUCTING COUNTERFACTUAL ESTIMATE UNDER CROSS-WORLD ASSUMPTIONS

Our goal is to construct a point estimate and prediction interval for the counterfactual outcome. If both $Y_i(1)$ and $Y_i(0)$ were observable for some individuals, the problem would reduce to classical regression with the factual outcome as an additional covariate. Since this is not possible, inferring counterfactual outcomes remains fundamentally challenging.

A natural starting point is to *separately* construct point estimates and prediction intervals for the treated group and the control group. For point prediction, any machine learning method, such as random forests or neural networks, can be used. For interval estimation, any conformal or other uncertainty quantification approach can be applied. We refer to Appendix A.2 for details on classical methods and their properties. Suppose their form is as follows:

$$\hat{\mu}_0(x) \text{ and } \hat{\mu}_1(x) \text{ are estimates of } \mu_0(x) \text{ and } \mu_1(x), \text{ respectively, and} \quad (3)$$

$$\tilde{C}_0(x) = [\hat{\mu}_0(x) - l_0(x), \hat{\mu}_0(x) + u_0(x)], \quad \tilde{C}_1(x) = [\hat{\mu}_1(x) - l_1(x), \hat{\mu}_1(x) + u_1(x)],$$

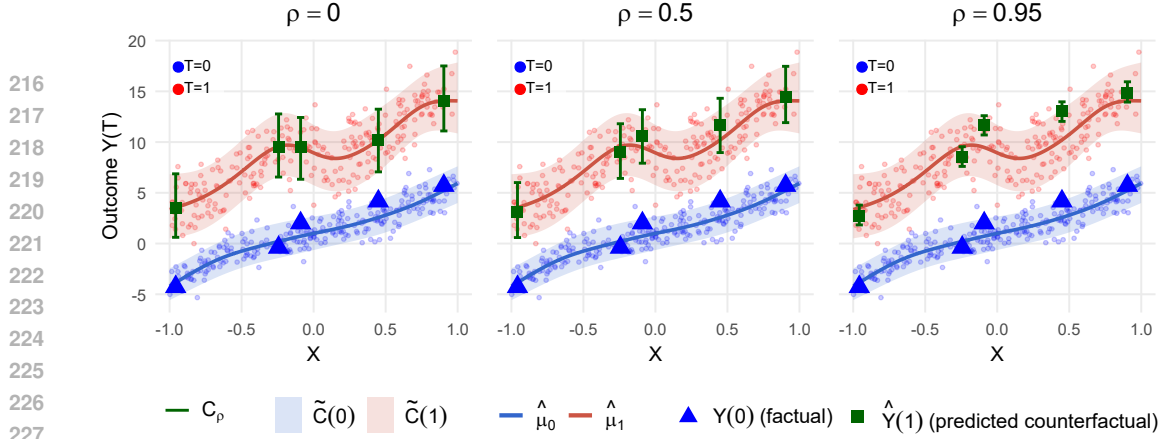


Figure 1: Proposed counterfactual estimator $\hat{Y}(1) := \hat{\mu}_\rho(x, y)$ and interval $C_\rho(x, y)$, combining baseline predictions with cross-world dependence. Here, $\rho = 0$ corresponds to ignoring the factual outcome, while $\rho = 1$ assumes perfect dependence. Illustrated on five highlighted units.

where $l_t, u_t \geq 0$ are the (lower and upper) widths of prediction intervals for $Y(t), t = 0, 1$. This is visualized in Figure 1. Ideally, \tilde{C}_t satisfy either marginal or conditional coverage:

$$P(Y(t) \in \tilde{C}_t(X)) \geq 0.9, \quad \text{or} \quad P(Y(t) \in \tilde{C}_t(x) \mid X = x) \geq 0.9,$$

where marginal coverage is automatically satisfied for conformal methods, while conditional coverage typically requires large sample sizes or strong assumptions in case of high-dimensional X . We combine these quantities to construct a point estimate $\hat{\mu}_\rho$ and a prediction interval C_ρ as follows:

Definition 2. Let $\rho \in [-1, 1]$. Consider baseline estimates in the form equation 3. We first define the point predictors:

$$\hat{\mu}_\rho^t(x, y) = \begin{cases} \hat{\mu}_1(x) + \rho \cdot \lambda(x) \cdot (y - \hat{\mu}_0(x)), & \text{if } t = 0, \\ \hat{\mu}_0(x) + \rho \cdot \frac{1}{\lambda(x)} \cdot (y - \hat{\mu}_1(x)), & \text{if } t = 1, \end{cases}$$

where $\lambda(x) = \frac{l_1(x) + u_1(x)}{l_0(x) + u_0(x)}$ is the relative width of the baseline prediction intervals. Given these point predictors, we define the C_ρ intervals by

$$C_\rho^t(x, y) = \begin{cases} \left[\hat{\mu}_\rho^t(x, y) - \sqrt{1 - \rho^2} \cdot l_1(x), \hat{\mu}_\rho^t(x, y) + \sqrt{1 - \rho^2} \cdot u_1(x) \right], & \text{if } t = 0, \\ \left[\hat{\mu}_\rho^t(x, y) - \sqrt{1 - \rho^2} \cdot l_0(x), \hat{\mu}_\rho^t(x, y) + \sqrt{1 - \rho^2} \cdot u_0(x) \right], & \text{if } t = 1. \end{cases}$$

For notational simplicity, we omit the superscript and write $C_\rho(x, y) = C_\rho^t(x, y)$ and $\hat{\mu}_\rho(x, y) = \hat{\mu}_\rho^t(x, y)$ when evident from context (typically when $t = 0$ and the counterfactual $Y(1)$ is of interest).

The choices for $\hat{\mu}_\rho$ and C_ρ are motivated by Theorem 1. The intuition is simple: the larger ρ , the more weight is put on the (centered) factual outcome. The role of $\lambda(x)$ is to adjust for potential differences in variance between treated and untreated groups; in settings where equal variances across groups can be reasonably assumed, one may simply set $\lambda(x) = 1$. While a claim of optimality in Theorem 1 is a strong statement, the result holds only under an idealized asymptotic scenario. In practice, estimation error or non-Gaussianity can lead to suboptimal performance, while additional assumptions can lead us to a different optimal prediction intervals. Nonetheless, the theorem provides valuable motivation: it shows that under ideal conditions, the C_ρ construction yields the smallest valid prediction set for a counterfactual.

3.1 CONSISTENCY

A direct consequence of Theorem 1 is that our estimators are consistent when the cross-world dependence between $Y(1)$ and $Y(0)$ is correctly specified.

270 **Theorem 2** (Asymptotic consistency of $\hat{\mu}_\rho$ and C_ρ). *Let $x \in \mathcal{X}$ and suppose $(Y(1), Y(0)) \mid X = x$ is Gaussian with $\rho = \text{cor}(Y(1), Y(0) \mid X = x) \in [-1, 1]$.*

273 *Let $\hat{\mu}_t(x)$ be consistent estimators of $\mu_t(x)$, and assume the prediction interval widths $l_t(x), u_t(x)$ are asymptotically conditionally valid¹ Then, for any fixed $y \in \mathbb{R}$: $\hat{\mu}_\rho(x, y)$ is a consistent estimator of the conditional mean,*

$$276 \quad \hat{\mu}_\rho(x, y) \xrightarrow{p} \mathbb{E}[Y(1) \mid X = x, Y(0) = y], \quad \text{as } n \rightarrow \infty.$$

278 *The C_ρ prediction intervals achieve asymptotic conditional coverage,*

$$279 \quad \lim_{n \rightarrow \infty} \mathbb{P}(Y(1) \in C_\rho(X, Y(0)) \mid X = x, Y(0) = y) = 0.9.$$

282 The assumption of Gaussianity and $\rho(x)$ are both modeling assumptions about how $Y(1)$ and $Y(0)$ relate, and neither can be learned from data. The Gaussian copula simply translates a chosen value of $\rho(x)$ into a fully specified cross-world distribution, and any other copula could serve the same role. This highlights the central challenge of retrospective counterfactual prediction: a full dependence structure between the two potential outcomes must be specified, not estimated. Analogous consistency and optimality results to Theorem 2 can be straightforwardly derived under any alternative cross-world dependence structure.

289 3.2 SPECIAL CASES: $\rho = 0$ AND $\rho = 1$

291 When $\rho = 0$, our predictions do not depend on y : $\mu_\rho(x, y) = \hat{\mu}_1(x)$ and $C_\rho(x, y) = \tilde{C}_1(x)$, as the 292 factual outcome $\tilde{Y}_1(0)$ provides no information about the missing potential outcome. The problem 293 then reduces to a standard regression setting, as discussed e.g. in Lei & Candès (2021). Under 294 $Y(1) \perp\!\!\!\perp Y(0) \mid X$, our C_ρ intervals inherit the validity of the baseline \tilde{C}_1 interval:

$$295 \quad \mathbb{P}(Y(1) \in \tilde{C}_1(X) \mid X = x) \geq 0.9 \implies \mathbb{P}(Y(1) \in C_\rho(X, Y(0)) \mid X = x, Y(0) = y) \geq 0.9. \quad (4)$$

297 Moreover, C_ρ is marginally valid even in finite samples, if \tilde{C}_1 is marginally valid (which holds if a 298 conformal method is used).

300 When $\rho = \pm 1$ and $\lambda(x) = 1$, we have $\hat{\mu}_\rho(x, y) = y + \hat{\tau}(x)$ and $C_\rho(x, y) = \{\hat{\mu}_\rho(x, y)\}$, corresponding 301 to a constant treatment effect:

$$302 \quad \mu_\rho(x, y_0) = \hat{\mu}_\rho(x, y_0) \implies \mathbb{P}(Y(1) \in C_\rho(X, Y(0)) \mid X = x, Y(0) = y) = 1. \quad (5)$$

304 In practice, however, $\mu_\rho(x, y_0)$ is unknown and must be estimated, introducing bias and potentially 305 non-valid prediction intervals. Section 3.3 discusses how to extend C_ρ intervals to account for the 306 additional uncertainty from this estimation.

308 3.3 FINITE SAMPLE BIAS CORRECTION: INTRODUCING C_ρ^{+CI} PREDICTION INTERVALS

309 We enlarge C_ρ prediction intervals by adding *confidence intervals* for μ_ρ , estimated for instance via 310 bootstrapping.

312 **Definition 3.** *Let $\rho \in [-1, 1]$. Consider prediction intervals for $Y(1)$ and $Y(0)$ of the form equation 313 3, and suppose we have confidence intervals $CI(x, y) = [\hat{\mu}_\rho(x, y) - r_l(x, y), \hat{\mu}_\rho(x, y) + 314 r_u(x, y)]$. We define the bias-corrected C_ρ^{+CI} intervals as*

$$315 \quad C_\rho^{+CI}(x, y) = \left[\hat{\mu}_\rho(x, y) - c \cdot r_l(x, y) - \sqrt{1 - \rho^2} \cdot l_{1-T_i}(x), \hat{\mu}_\rho(x, y) + c \cdot r_u(x, y) + \sqrt{1 - \rho^2} \cdot u_{1-T_i}(x) \right],$$

317 where $l_{1-T_i}(x)$ and $u_{1-T_i}(x)$ select the appropriate prediction bounds depending on treatment 318 status T_i , and $c \in [0, 1]$ is a hyperparameter. In simple terms, C_ρ^{+CI} extends C_ρ by adding a scaled 319 confidence interval around $\hat{\mu}_\rho(x, y)$, with scaling factor c . We consider the choice $c = \rho^2$ following 320 the same argument as in (Bodik et al., 2025).

322 ¹This holds for many nonparametric estimators under mild smoothness assumptions, including random 323 forests for estimating $\hat{\mu}_t(x)$ and CQR using quantile random forests for prediction intervals. More details are given in Appendix D.

Following equation 4 and equation 5, when $\rho = 0$, no adjustment is needed, while for $\rho = \pm 1$, full confidence intervals must be incorporated to guarantee correct coverage. This motivates the choice $c = \rho^2$, ensuring that C_ρ^{+CI} smoothly interpolates between no correction ($\rho = 0$) and full correction ($\rho = 1$). For this choice, we also have the following guarantee.

Consequence 1. *If $\rho = \pm 1$ and confidence intervals satisfy $\mathbb{P}(\mu(x, y_0) \in \hat{\mu}_\rho(x, y_0) \pm r(x, y_0)) \geq 1 - \alpha$, then $\mathbb{P}(Y(1) \in C_\rho^{+CI}(X, Y(0)) \mid X = x, Y(0) = y) \geq 1 - \alpha$.*

4 NUMERICAL EXPERIMENTS

We evaluate our method on synthetic, semi-synthetic, and real datasets using both point estimation and prediction interval metrics, comparing against four baselines under varying cross-world correlation ρ . A user-friendly implementation of our methods in both R and Python, along with scripts to reproduce all experiments, is available at: [github link anonymized for review].

4.1 DETAILS

Datasets: We consider a variety of data-generating processes commonly used in the related literature; full details are provided in Appendix C.1. The **synthetic** datasets feature non-constant propensity scores and randomly generated CATE functions based on smooth random polynomials. These settings allow us to vary the dimensionality $d = \dim(\mathbf{X})$ and the cross-world correlation parameter ρ , thus controlling both complexity and treatment-effect heterogeneity. In addition, we include the **IHDP** dataset, which uses real covariates from a randomized trial and simulated counterfactual outcomes, providing a semi-synthetic benchmark. The **Twins** dataset contains real covariates and real paired outcomes corresponding to different treatment assignments, enabling the construction of both factual and counterfactual outcomes for each unit.

Implementation details: To better reflect real-world scenarios where ρ is unknown, we report both i) $\rho_{used} = \rho_{true}$ and ii) $\rho_{used} = \rho_{true} + Unif(-0.5, 0.5)$ capped at $[-1, 1]$.

To construct the proposed C_ρ and C_ρ^{+CI} intervals, we use CQR (see Appendix A.2) to produce the base intervals in equation 3. While more advanced methods often achieve better empirical results, we adopt CQR as a simple, well-established baseline, following Lei & Candès (2021); Alaa et al. (2023), and Bodik et al. (2025).

Our algorithm jointly estimates conditional means and quantiles: in low dimensions ($d \leq 5$) we use GAM for the mean and qGAM (Fasiolo et al., 2017) for quantiles, while in higher dimensions ($d > 5$) we switch to random forests for the mean and quantile random forests (Meinshausen & Ridgeway, 2006) for quantiles, trading some low-dimensional efficiency for scalability. TabPFN (Hollmann et al., 2023) is a good potential alternative.

Baseline methods: In Appendix A.1, we provide details of the existing methods used to estimate counterfactuals. We consider four representative approaches. First, **CATE-adjusted imputation** estimates the CATE via a T-learner (Künzel et al., 2019), DR-learner (doubly robust, Dukes et al. (2024)) or Generalized Random Forest (Athey et al., 2019), and adjusts the observed outcome using $\hat{Y}_i(1) = Y_i(0) + \hat{\tau}(X_i)$. We only report the T-learner as it yielded the best results on the considered datasets. Note that while many other CATE estimators exist, the goal is to illustrate the core imputation approach, which remains fundamentally limited even with perfectly estimated CATE. Second,

Direct Outcome (DO) modeling fits the treatment-specific regression $\hat{Y}_i(1) := \mu_1(X_i)$ using Random Forests (Wager & Athey, 2018) or Generalized Additive Models (Fasiolo et al., 2017) (using the same choices as in C_ρ). Third, **Matching-based imputation** uses nearest-neighbor matching with Mahalanobis distance to impute the missing potential outcome from similar units in the opposite treatment group. Fourth, **adversarial generative modeling** employs GANITE (Yoon et al., 2018), a two-stage generative adversarial network that imputes and refines counterfactual predictions, typically suitable only in high-dimensional, nonlinear settings.

Setup: We conducted experiments on datasets: synthetic ($n = 1000$), IHDP ($n = 747$), and Twins ($n = 11,983$). Each synthetic and IHDP experiment was repeated 50 times to reduce Monte Carlo variability, while the Twins dataset was analyzed once using the full sample. All methods used an 80/20 train-calibration split for CQR and prediction intervals at level $\alpha = 0.1$. Computing μ_ρ and C_ρ is fast, as the main cost lies in fitting four quantile regressions; however, C_ρ^{+CI} requires

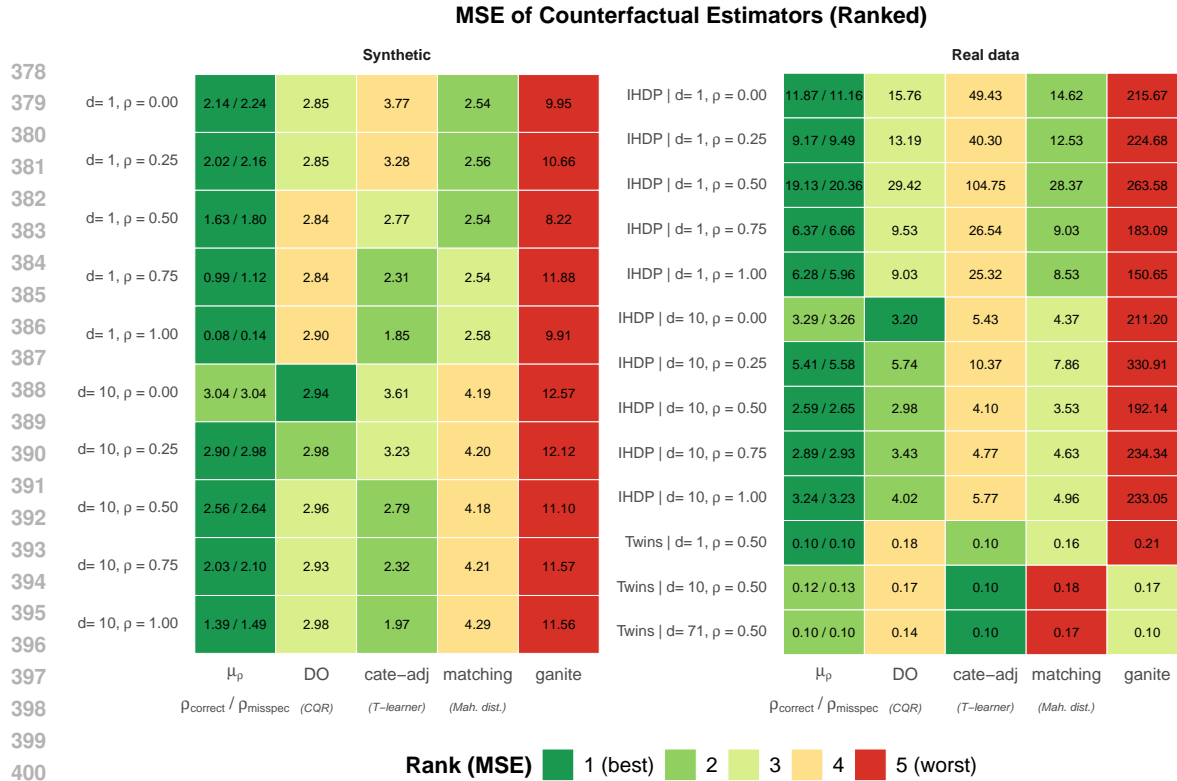


Figure 2: Mean squared error of different estimators across different datasets, averaged over 50 repetitions. In μ_p , we use either $\rho = \rho_{true}$, or mimic misspecification by using $\rho = \rho_{true} + Unif(-0.5, 0.5)$. Standard deviations for each entry can be found in Appendix B.

computing bootstrap confidence intervals (we used 100 bootstraps), which is computationally more intensive; running all datasets and repetitions took approximately four days on an Intel Core i5-6300U (2.5 GHz, 16 GB RAM).

410 **Metrics:** To assess performance, we use MSE for point predictions and the Interval Score (metric
411 that combines coverage and width) for prediction intervals:

$$\text{MSE} = \frac{1}{n} \sum_{i=1}^n (\hat{Y}_i^{cf} - Y_i^{cf})^2, \quad \text{IS}_{\alpha} = \frac{1}{n} \sum_{i=1}^n (U_i - L_i) + \frac{2}{\alpha} [(L_i - Y_i^{cf})_+ + (Y_i^{cf} - U_i)_+],$$

where $[L_i, U_i]$ are the estimated prediction intervals at level $1 - \alpha$ and $z_+ = \max(z, 0)$.

4.2 RESULTS OF THE EXPERIMENTS

Figure 2 presents the MSE results of point predictions; Figure 5 in Appendix C.2 presents the interval scores for prediction intervals. Both of the variants (correctly specified ρ and misspecified ρ) strongly outperform other methods in scenarios where $\rho \neq 0$ or 1; if $\rho = 0$ note that DO have almost identical performance as our method. If $\rho = 1$, the CATE-adjusted estimators have competitive performance.

While it seems that GANITE has very bad performance, note that it was built for large dimensional problems, and for large d and n it would perform often better. Our method is more suitable for low dimensions, when the factual $Y(T)$ contains significant information beyond the information in the observed covariates.

429 In a few real-world datasets, ρ_{misspec} yields slightly better performance than ρ_{correct} , a consequence
 430 of Monte Carlo variability. As shown in Figure 5, the corresponding confidence intervals are large
 431 in these cases, and resolving these differences would require hundreds of repetitions to reduce sim-
 ulation noise.

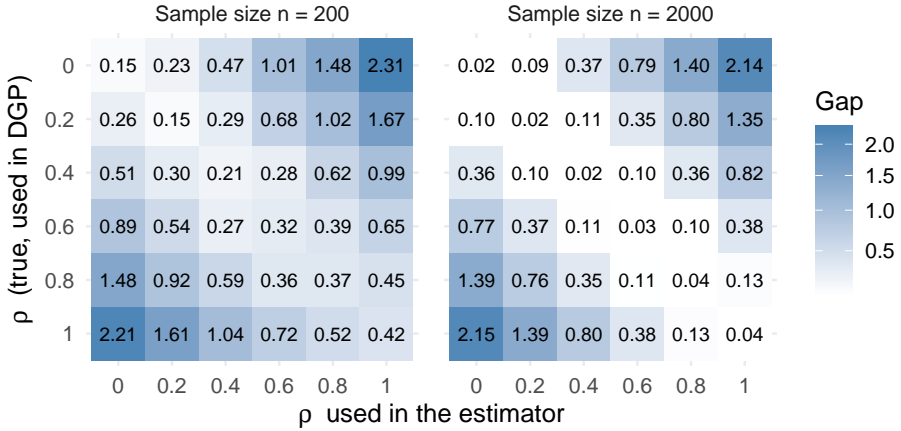


Figure 3: Gap = $\text{MSE}_{\text{our}} - \text{MSE}_{\text{oracle}}$ calculated across different misspecifications of ρ . Bias persists when ρ is far from the truth, but vanishes asymptotically if ρ is specified correctly. This demonstrates that incorporating even approximate knowledge of cross-world dependence improves counterfactual predictions.

4.3 ADDITIONAL EXPERIMENTS: MISSPECIFIED ρ AND NON-GAUSSIANITY

We conduct two additional experiments, evaluating the Gap = $\text{MSE}_{\text{our}} - \text{MSE}_{\text{oracle}}$, where the oracle estimator is equal to the true $\mathbb{E}[Y^{cf} | X, Y^{obs}, T]$. All details can be found in Appendix B.

- **(Misspecifying ρ).** Figure 3 reports experiments on synthetic data varying the *true* correlation ρ_{true} in the data-generating process (DGP) and the *assumed* value ρ_{est} in our estimator. Bias grows with misspecification $|\rho_{\text{est}} - \rho_{\text{true}}|$, and vanishes with larger n only when ρ_{est} is close to ρ_{true} ; otherwise, it persists even asymptotically. This shows that even rough knowledge of ρ yields large gains over ignoring the factual outcome.
- **(Robustness to non-Gaussianity).** Appendix B.1 (Figure 4) contains experiments with non-Gaussian outcome distributions ($Y(0), Y(1)$). In all cases the gap vanishes with n , though convergence is slower under non-Gaussian noise. Discrepancies are most visible at $\rho = 1$.

5 CONCLUSION AND FUTURE RESEARCH

The factual outcome carries valuable individual-level information that should not be ignored in counterfactual prediction. We formalize the importance of the factual outcome through the cross-world correlation parameter ρ , which determines how strongly observed and unobserved outcomes are linked. By treating ρ as an explicit modeling choice, our approach interpolates between classical extremes, with $\rho = 0$ discarding the factual outcome and $\rho = 1$ assuming constant effects, and delivers predictions that are theoretically well motivated and empirically effective whenever even approximate knowledge of ρ is available.

Although ρ is not identifiable from observed data, *every existing method already makes a fixed, implicit assumption about ρ* . Our contribution is to make this dependence explicit, enabling practitioners to incorporate domain knowledge or sensitivity analysis into counterfactual inference. This transparency clarifies the assumptions underlying prediction and opens new possibilities for modeling cross-world dependence.

Future work should explore richer dependence structures, such as copula-based models, which would enable a broader class of assumptions about how potential outcomes co-vary. This would yield a more general framework for counterfactual prediction, accommodating settings where simple correlation is inadequate. Another promising direction is to extend the methodology to continuous treatments or dynamic settings such as time series, where cross-world assumptions could provide structure for dose-response curves or evolving interventions, thereby enhancing both interpretability and stability. Beyond methodological extensions, future research may also investigate applications in domains where expert knowledge about cross-world dependence is available, such as medicine, economics, or climate science.

486 REPRODUCIBILITY STATEMENT AND USAGE OF LARGE LANGUAGE MODELS
487

488 All code and datasets used in this work are provided in the supplementary material to ensure full
489 reproducibility of our results. We declare that we used a large language model for grammar and
490 language polishing, as well as for limited coding assistance (e.g., boilerplate code and debugging).
491 All conceptual and theoretical contributions, experimental designs, and conclusions are our own.
492

493 REFERENCES
494

495 A. Abadie and G. Imbens. Large sample properties of matching estimators for average treatment
496 effects. *Econometrica*, 2006.

497 A. Agarwal, M. Xiao, R. Barter, O. Ronen, B. Fan, and B. Yu. PCS-UQ: Uncertainty quantification
498 via the predictability-computability-stability framework, 2025. URL <https://arxiv.org/abs/2505.08784>.

500 A. Alaa and M. van der Schaar. Bayesian inference of individualized treatment effects using
501 multi-task gaussian processes. In *Advances in Neural Information Processing Systems*, volume 30, 2017.
502 URL https://proceedings.neurips.cc/paper_files/paper/2017/file/6a508a60aa3bf9510ea6acb021c94b48-Paper.pdf.

503 A. Alaa, Z. Ahmad, and M. van der Laan. Conformal meta-learners for predictive inference of
504 individual treatment effects. In *Thirty-seventh Conference on Neural Information Processing
505 Systems*, 2023. URL <https://openreview.net/forum?id=IwnINorSZ5>.

506 R. M. Andrews and V. Didelez. Insights into the cross-world independence assumption of causal
507 mediation analysis. *Epidemiology*, 32(2):209–219, 2021. doi: 10.1097/EDE.0000000000001313.

508 A. N. Angelopoulos, R. F. Barber, and S. Bates. Theoretical foundations of conformal prediction,
509 2024. URL <https://arxiv.org/abs/2411.11824>.

510 S. Athey, J. Tibshirani, and S. Wager. Generalized random forests. *The Annals of Statistics*, 47(2):
511 1148–1178, 2019.

512 I. Azizi, J. Bodik, J. Heiss, and B. Yu. Clear: Calibrated learning for epistemic and aleatoric risk,
513 2025. URL <https://arxiv.org/abs/2507.08150>.

514 K. Bairaktari, R. Izbicki, and E. J. Candès. Kandinsky conformal prediction: Beyond class- and
515 covariate-conditional coverage. In *Proceedings of the 42nd International Conference on Machine
516 Learning (ICML)*, 2025. URL <https://arxiv.org/abs/2502.17264>.

517 R. F. Barber, E. J. Candès, A. Ramdas, and R. J. Tibshirani. The limits of distribution-free condi-
518 tional predictive inference, 2020. URL <https://arxiv.org/abs/1903.04684>.

519 I. Bica, J Jordon, and M van der Schaar. Estimating the effects of continuous-valued interventions us-
520 ing generative adversarial networks. In H. Larochelle, M. Ranzato, R. Hadsell, M.F. Balcan, and
521 H. Lin (eds.), *Advances in Neural Information Processing Systems*, volume 33, pp. 16434–16445.
522 Curran Associates, Inc., 2020. URL https://proceedings.neurips.cc/paper_files/paper/2020/file/bea5955b308361a1b07bc55042e25e54-Paper.pdf.

523 J. Bodik and V. Chavez-Demoulin. Structural restrictions in local causal discovery: identifying direct
524 causes of a target variable. *Biometrika*, 2025. URL <https://arxiv.org/abs/2307.16048>.

525 J. Bodik, Y. Huang, and B. Yu. Cross-world assumption and refining prediction intervals for individ-
526 ual treatment effects. *ArXiv preprint ArXiv:2507.12581*, 2025. URL <https://arxiv.org/abs/2507.12581>.

527 M. Cai, S. Buuren, and V. Gerk. How to relate potential outcomes: Estimating individual treatment
528 effects under a given specified partial correlation, 2022. URL <https://arxiv.org/abs/2208.12931>.

540 K. E. Colson et al. Optimizing matching and analysis combinations for estimating causal effects.
 541 *Scientific Reports*, 2016.

542

543 A. Dieng et al. Interpretable almost-exact matching for causal inference. *Journal of Causal Inference*, 2019.

544

545 P. Ding and F. Li. Causal inference: A missing data perspective. *Statistical Science*, 33(2):214–237,
 546 2018. doi: 10.1214/18-STS645. URL <https://doi.org/10.1214/18-STS645>.

547

548 P. Ding, A. Feller, and L. Miratrix. Decomposing treatment effect variation. *Journal of the American
 549 Statistical Association*, 114(525):304–317, 2019.

550

551 O. Dukes, S. Vansteelandt, and D. Whitney. On doubly robust inference for double machine learning
 552 in semiparametric regression. *Journal of Machine Learning Research*, 25(279):1–46, 2024. URL
 553 <http://jmlr.org/papers/v25/22-1233.html>.

554

555 Y. Fan and S. S. Park. Sharp bounds on the distribution of treatment effects and their statistical
 556 inference. *Econometric Theory*, 26(3):931–951, 2010. doi: 10.1017/S026646609990168.

557

558 M. Fasiolo, Y. Goude, R. Nedellec, and S. Wood. Fast calibrated additive quantile regression, 2017.
 Available at <https://arxiv.org/abs/1707.03307>.

559

560 S. P. Firpo. Efficient semiparametric estimation of quantile treatment effects. *Econometrica*, 75(1):
 259–276, 2007.

561

562 I. Gibbs, J. J. Cherian, and E. J. Candès. Conformal prediction with conditional guarantees. *Journal
 563 of the Royal Statistical Society Series B: Statistical Methodology*, pp. qkaf008, 03 2025. ISSN
 564 1369-7412. doi: 10.1093/rssb/qkaf008. URL [https://doi.org/10.1093/rssb/
 565 qkaf008](https://doi.org/10.1093/rssb/qkaf008).

566

567 J. J. Heckman, J. Smith, and N. Clements. Making the most out of program evaluations and social
 568 experiments: Accounting for heterogeneity in program impacts. *Review of Economic Studies*, 64
 (4):487–535, 1997.

569

570 J. L. Hill. Bayesian nonparametric modeling for causal inference. *Journal of Computational and
 571 Graphical Statistics*, 20(1):217–240, 2011. doi: 10.1198/jcgs.2010.08162.

572

573 N. Hollmann, S. Müller, K. Eggensperger, and F. Hutter. TabPFN: A transformer that solves small
 574 tabular classification problems in a second, 2023. URL [https://arxiv.org/abs/2207.
 575 01848](https://arxiv.org/abs/2207.01848).

576

577 Y. Hur and T. Liang. A convexified matching approach to imputation and individualized inference,
 2024. URL <https://arxiv.org/abs/2407.05372>.

578

579 G. W. Imbens and D. B. Rubin. *Causal Inference for Statistics, Social, and Biomedical Sciences: An
 580 Introduction*. Cambridge University Press, Cambridge, 2015. doi: 10.1017/CBO9781139025751.

581

582 F. Johansson, U. Shalit, and D. Sontag. Learning representations for counterfactual inference. In
 583 *Proceedings of The 33rd International Conference on Machine Learning*, volume 48 of *Proceedings of Machine Learning Research*, pp. 3020–3029, New York, New York, USA, 20–22 Jun
 2016. PMLR. URL <https://proceedings.mlr.press/v48/johansson16.html>.

584

585 J. Jonkers, J. Verhaeghe, G. Wallendael, L. Duchateau, and S. Hoecke. Conformal convolution and
 586 monte carlo meta-learners for predictive inference of individual treatment effects, 2024. URL
 587 <https://arxiv.org/abs/2402.04906>.

588

589 S. Joshi, A. Korba, T. Trogdon, and E. Candès. Conformal inference under high-dimensional co-
 590 variate shifts via likelihood-ratio regularization. *arXiv preprint arXiv:2502.13030*, 2025. URL
 591 <https://arxiv.org/abs/2502.13030>.

592

593 N. Kallus. A Framework for Optimal Matching for Causal Inference. In Aarti Singh and Jerry Zhu
 (eds.), *Proceedings of the 20th International Conference on Artificial Intelligence and Statistics*,
 594 volume 54 of *Proceedings of Machine Learning Research*, pp. 372–381. PMLR, 20–22 Apr 2017.

594 K. Kasa, A. Ranganath, and Á. Cuevas. Adapting prediction sets to distribution shifts without
 595 labels. In *International Conference on Learning Representations (ICLR)*, 2025. URL <https://openreview.net/forum?id=k2gGy2hpx>.

596

597 K. Kim. Semiparametric counterfactual regression. *arXiv preprint arXiv:2504.02694*, 2025.

598

599 K. Kim, E. H. Kennedy, and J. R. Zubizarreta. Doubly robust counterfactual classification. In
 600 *Advances in Neural Information Processing Systems*, volume 35, pp. 34831–34845, 2022.

601

602 S. R. Künzel, J. S. Sekhon, P. J. Bickel, and B. Yu. Metalearners for estimating heterogeneous
 603 treatment effects using machine learning. *Proceedings of the National Academy of Sciences*, 116
 604 (10):4156–4165, 2019.

605

606 A. Lacombe and M. Sebag. Asymmetrical latent representation for individual treatment effect mod-
 607 eling, 2025. URL <https://arxiv.org/abs/2501.14006>.

608

609 L. Lei and E. J. Candès. Conformal inference of counterfactuals and individual treatment ef-
 610 fects. *Journal of the Royal Statistical Society Series B: Statistical Methodology*, 83(5):911–938,
 November 2021. doi: 10.1111/rssb.12445.

611

612 F. Li, P. Ding, and F. Mealli. Bayesian causal inference: A critical review, 2022. URL <https://arxiv.org/abs/2206.15460>.

613

614 C. Louizos, U. Shalit, J. Mooij, D. Sontag, R. Zemel, and M. Welling. Causal effect inference
 615 with deep latent-variable models. In *Proceedings of the 31st International Conference on Neural
 616 Information Processing Systems*, NIPS’17, pp. 6449–6459, 2017.

617

618 A. McClean, Z. Branson, and E. H. Kennedy. Nonparametric estimation of conditional incremental
 619 effects. *Journal of Causal Inference*, 12(1):20230024, 2024. doi: 10.1515/jci-2023-0024.

620

621 N. Meinshausen and G. Ridgeway. Quantile regression forests. *Journal of Machine Learning Re-
 622 search*, 7(6), 2006.

623

624 R. B. Nelsen, J. Quesada-Molina, J. Antonio Rodríguez-Lallena, and M. Úbeda Flores. Bounds on
 625 bivariate distribution functions with given margins and measures of association. *Communications
 in Statistics - Theory and Methods*, 30(6):1055–1062, 2001. doi: 10.1081/STA-100104355.

626

627 J. Pearl and D. Mackenzie. *The Book of Why*. Penguin Books, 2019. URL <http://bayes.cs.ucla.edu/WHY/>.

628

629 K. Perlin. An image synthesizer. *Siggraph Comput. Graph.*, 19(0097-8930):287–296, 1985.

630

631 V. Plassier, O. Bouhali, and N. El Karoui. Rectifying conformity scores for better conditional cov-
 632 erage. *arXiv preprint arXiv:2502.16336*, 2025. URL <https://arxiv.org/abs/2502.16336>.

633

634 Y. Romano, E. Patterson, and E. Candès. Conformalized quantile regression. In *Advances in Neural
 635 Information Processing Systems*, pp. 3538–3548, 2019.

636

637 D. Rubin. Causal inference using potential outcomes. *Journal of the American Statistical Associa-
 638 tion*, 100(469):322–331, 2005. doi: 10.1198/016214504000001880.

639

640 D. B. Rubin. Comment: Neyman (1923) and causal inference in experiments and observational
 641 studies. *Statistical Science*, 5(4):472–480, November 1990. doi: 10.1214/ss/1177012032.

642

643 E. A. Stuart. Matching methods for causal inference: A review and a look forward. *Statistical
 644 Science*, 2010.

645

646 R. J. Tibshirani, R. F. Barber, E. Candès, and A. Ramdas. Conformal prediction under covariate
 647 shift. *Advances in Neural Information Processing Systems*, pp. 2530–2540, 2019.

648

649 V. Vovk, A. Gammerman, and G. Shafer. *Algorithmic Learning in a Random World*. Springer
 650 Science & Business Media, 2005.

648 S. Wager. Causal inference: A statistical learning approach, 2024. URL https://web.stanford.edu/~swager/causal_inf_book.pdf. Stanford University.

649

650

651 S. Wager and S. Athey. Estimation and inference of heterogeneous treatment effects using random

652 forests. *Journal of the American Statistical Association*, 113(523):1228–1242, 2018.

653 B. Wang and X. Qiao. Conformal prediction under generalized covariate shift with posterior drift.

654 In *Proceedings of the 28th International Conference on Artificial Intelligence and Statistics (AIS-*

655 *TATS*), 2025. URL <https://arxiv.org/abs/2502.17744>.

656

657 R. W. Wright. Causation in tort law. *California Law Review*, 73(6):1735–1828, 1985. doi: 10.2307/

658 3480056.

659 L. Yao, S. Li, Y. Li, M. Huai, J. Gao, and A. Zhang. Representation learning for

660 treatment effect estimation from observational data. In *Advances in Neural In-*

661 *formation Processing Systems*, volume 31. Curran Associates, Inc., 2018. URL

662 https://proceedings.neurips.cc/paper_files/paper/2018/file/a50abba8132a77191791390c3eb19fe7-Paper.pdf.

663

664 J. Yoon, J. Jordon, and M. van der Schaar. GANITE: Estimation of individualized treatment effects

665 using generative adversarial nets. In *International Conference on Learning Representations*, 2018.

666 URL <https://openreview.net/forum?id=ByKWUeWA->.

667

668 B. Yu and R. L. Barter. *Veridical Data Science: The Practice of Responsible Data Analysis and*

669 *Decision Making*. Adaptive Computation and Machine Learning Series. MIT Press, 2024. ISBN

670 0262379708, 9780262379700.

671 Z. Zhang and T. S. Richardson. Bounds on the distribution of a sum of two random variables:

672 Revisiting a problem of kolmogorov with application to individual treatment effects, 2025a. URL

673 <https://arxiv.org/abs/2405.08806>.

674

675 Z. Zhang and T. S. Richardson. Individual treatment effect: Prediction intervals and sharp bounds,

676 2025b. URL <https://arxiv.org/abs/2506.07469>.

677

678

679

680

681

682

683

684

685

686

687

688

689

690

691

692

693

694

695

696

697

698

699

700

701

702
 703
 704
Appendix

705
A LITERATURE REVIEW: DETAILS

707
A.1 COUNTERFACTUAL ESTIMATION METHODS: OTHER APPROACHES

709
 710
 We consider four classes of approaches for estimating the unobserved potential outcome $Y_i(1)$ for
 units with $T_i = 0$ (and analogously $Y_i(0)$ for $T_i = 1$).

711
CATE-adjusted imputation (CATE-adj). This approach first estimates CATE $\tau(X_i)$ and then
 712 shifts the observed control outcome by this estimated effect:

714

$$\hat{Y}_i(1) = Y_i(0) + \hat{\tau}(X_i).$$

715
 We use three alternative CATE estimators: the T-learner (Künzel et al., 2019), the Generalized
 716 Random Forest (GRF) (Athey et al., 2019), and a doubly robust (DR) estimator (Dukes et al., 2024).
 717 Closely related meta-learners include the S-learner, which fits a single model with treatment as an
 718 input feature, and the X-learner, which augments the T-learner with imputed treatment effects for the
 719 opposite treatment group and often performs well under treatment imbalance (Künzel et al., 2019).
 720 These alternative meta-learners share the same conceptual foundation. Johansson et al. (2016);
 721 Lacombe & Sebag (2025) use deep learning alternatives; balancing counterfactual regression or
 722 adding assymetrical latend represnetation.

723
 To quantify uncertainty, confidence intervals are computed using standard procedures, obtaining
 724 prediction intervals in a form $\hat{Y}_i(1) = Y_i(0) + \hat{\tau}(X_i) \pm \text{conf.int}(\hat{\tau}(X_i))$. In our experiments, we only
 725 considered T-learner, GRF and DR estimators for CATE-adjusted imputation, as other approaches
 726 are typically significantly more performative only in high-dimensional datasets or when treated and
 727 untreated units differ substantially, which is not the case in our datasets.

729
Direct outcome modeling (DO). Here we model the treatment-specific regression function
 730 $\mu_1(x) = \mathbb{E}[Y | X = x, T = 1]$ directly from the treated sample and use $\hat{Y}_i(1) = \hat{\mu}_1(X_i)$ for coun-
 731 terfactual prediction. We consider two implementations: Random Forests (RF) (Wager & Athey,
 732 2018) and Generalized Additive Models (GAM) (Fasiolo et al., 2017). Unlike the CATE-adjusted
 733 approach, these methods do not require access to the observed control outcome $Y_i(0)$ for the unit,
 734 relying entirely on model-based extrapolation from treated units. To quantify uncertainty, we use
 735 the same prediction intervals as in equation 3.

736
 There is also a large number of similar approaches besides RF and GAM, also adjusting for the
 737 distribution shift between the treated/untreated groups. Yao et al. (2018) employ deep representation
 738 learning to estimate $\hat{Y}_i(1-T) = g(f(X_i), T_i)$ where f, g are neural networks based preserving local
 739 similarity between the treated groups.

741
Matching-based imputation (Matching). This approach imputes missing potential outcomes us-
 742 ing outcomes from similar units in the opposite treatment group, selected via a distance metric
 743 in covariate space (Stuart, 2010; Abadie & Imbens, 2006). Beyond nearest-neighbor and optimal
 744 matching, advances include kernel-based matching to minimize estimation error (Kallus, 2017) and
 745 full or genetic matching combined with double-robust analysis for improved bias and efficiency
 746 (Colson et al., 2016). For high-dimensional or categorical data, algorithms like DAME prioritize
 747 relevant covariates (Dieng et al., 2019). Similar ideology was also used in ALRITE (Lacombe &
 748 Sebag, 2025), where the authors imputed counterfactuals based on the closest distance in a latent
 749 space, in order to improve CATE estimation.

750
 We implemented nearest-neighbor matching with a uniform kernel and optional replacement, using
 751 either the Mahalanobis distance between standardized covariates or the absolute difference in logit
 752 propensity scores (the former led to better results so we only report that). The propensity scores
 753 is estimated by standard classification forest. For a treated unit, the counterfactual $\hat{Y}_i(0)$ is the
 754 average outcome among its matched controls, and vice versa for control units. This nonparametric
 755 approach relies on local overlap in covariates and assumes conditional independence of potential
 outcomes and treatment given covariates. To quantify uncertainty, we construct unit-level prediction

756 intervals for the counterfactuals using the empirical variance of the donor outcomes: for a unit with
 757 $K \geq 2$ matches, the half-width is given by $t1 - \alpha/2, K - 1 \cdot s/\sqrt{K}$, where s is the sample standard
 758 deviation of the matched donor outcomes, yielding $(\hat{Y}_i^{\text{cf}} \pm \text{half-width})$; if $K = 1$, the half-width
 759 is zero. This approach implicitly assumes conditional independence of potential outcomes ($\rho = 0$),
 760 similarly to DO and independent treatment given covariates.
 761

762 **Adversarial generative modeling (GANITE).** GANITE (Yoon et al., 2018) employs a two-stage
 763 generative adversarial network (GAN) framework tailored to causal inference. In the first stage,
 764 a generator–discriminator pair is trained to impute the missing counterfactual outcomes by making
 765 the generated outcomes indistinguishable from observed ones given covariates and treatment assign-
 766 ment. In the second stage, a separate adversarial network refines these predictions to improve estima-
 767 tion of individualized treatment effects, encouraging accurate recovery of both potential outcomes
 768 simultaneously. This approach is particularly suited to high-dimensional, nonlinear settings. Some
 769 extinctions were also proposed that work better under some alternative scenarios (e.g. SCIGAN-ITE
 770 by Bica et al. (2020)).

771 **Other approaches.** Some other approaches exist, such as **Bayesian causal inference**, where
 772 the missing counterfactuals are treated as latent variables, and uncertainty is integrated through the
 773 posterior distribution. For example, Alaa & van der Schaar (2017) propose a Bayesian multitask
 774 Gaussian process to jointly model $(Y(1), Y(0)) | X$, producing posterior distributions over the po-
 775 tential outcomes. While Bayesian methods offer coherent uncertainty quantification, they often rely
 776 on strong modeling assumptions and can be sensitive to prior specifications (Li et al., 2022). More-
 777 over, they can be restrictive when aiming to leverage flexible modern machine learning techniques.
 778

779 A.2 UNCERTAINTY QUANTIFICATION AND PREDICTION INTERVALS IN CLASSICAL 780 REGRESSION

781 In a standard regression framework, we observe data $(X_i, Y_i) \sim P_X \times P_{Y|X}$ for $i = 1, \dots, n$, and
 782 seek a prediction set $C(X)$ for future responses that satisfies a coverage property. Two common
 783 notions of coverage are:

$$784 \mathbb{P}(Y_{n+1} \in C(X_{n+1})) \geq 1 - \alpha \quad (\text{marginal coverage}), \\ 785 \mathbb{P}(Y_{n+1} \in C(X_{n+1}) | X_{n+1} = x) \geq 1 - \alpha \quad (\text{conditional coverage}). \\ 786$$

787 Conditional coverage is a stronger requirement but is generally unattainable in a distribution-free,
 788 finite-sample setting without strong assumptions or asymptotics (Barber et al., 2020). By contrast,
 789 marginal coverage can be attained without modeling assumptions via conformal prediction (An-
 790 gelopoulos et al., 2024). Recent work has also explored data-driven techniques to improve condi-
 791 tional coverage, such as combining epistemic+aleatoric sources of uncertainty (Azizi et al., 2025),
 792 rectifying conformity scores (Plassier et al., 2025), or optimizing subgroup-conditional guarantees
 793 through flexible frameworks like Kandinsky conformal prediction (Bairaktari et al., 2025). These
 794 developments are consistent with the broader principles of Predictability, Computability, and Stabil-
 795 ity (PCS) advocated for trustworthy data science (Agarwal et al., 2025; Yu & Barter, 2024).

796 Conformal methods produce prediction intervals with exact finite-sample marginal coverage under
 797 exchangeability of the observed and future data points (Vovk et al., 2005; Angelopoulos et al., 2024).
 798 These methods typically split the data into training and calibration subsets, construct a preliminary
 799 predictor on the training set, and adjust it on the calibration set to guarantee coverage. A prominent
 800 example is Conformalized Quantile Regression (CQR), which uses estimated conditional quantiles
 801 to build tighter prediction intervals (Romano et al., 2019).

802 **Estimation procedure for CQR.** The key idea of CQR is to combine quantile regression with
 803 conformal calibration:

- 804 1. **Split the data.** Randomly divide the dataset into a training set $\mathcal{D}_{\text{train}}$ and a calibration set
 $\mathcal{D}_{\text{calib}}$. The split fraction is typically 80/20.
- 805 2. **Fit quantile regression models.** On $\mathcal{D}_{\text{train}}$, estimate the conditional lower and upper quan-
 $\text{tile functions } \hat{q}_{\alpha/2}(x) \text{ and } \hat{q}_{1-\alpha/2}(x)$, often quantile random forest (Meinshausen & Ridge-
 $\text{way, 2006), qGAM (Fasiolo et al., 2017) or neural networks to approximate conditional}$
 $\text{quantiles for levels } \alpha/2 \text{ and } 1 - \alpha/2.$

810
 811 3. **Compute conformity scores.** For each $(X_i, Y_i) \in \mathcal{D}_{\text{calib}}$, compute the nonconformity
 812 score:

$$s_i = \max\{\hat{q}_{\alpha/2}(X_i) - Y_i, Y_i - \hat{q}_{1-\alpha/2}(X_i), 0\}.$$

813 This measures how far Y_i lies outside the estimated conditional quantile interval.
 814

815 4. **Calibrate using empirical quantiles.** Let $Q_{1-\alpha}(s_1, \dots, s_m)$ be the $(1 - \alpha)$ -empirical
 816 quantile of the scores from the calibration set ($m = |\mathcal{D}_{\text{calib}}|$).
 817 5. **Construct prediction intervals.** For a new point x , the CQR prediction set is:

$$\tilde{C}(x) = [\hat{q}_{\alpha/2}(x) - Q_{1-\alpha}, \hat{q}_{1-\alpha/2}(x) + Q_{1-\alpha}].$$

820 This adjustment ensures that the final interval achieves marginal coverage at level $1 - \alpha$ in finite
 821 samples under exchangeability, while leveraging conditional quantile estimates for tighter intervals.
 822

823 However, exchangeability (slightly weaker assumption than i.i.d.) can fail in the presence of covariate
 824 shift, e.g., in observational studies comparing treated and untreated units. In such settings, even
 825 defining marginal coverage requires specifying the *target covariate distribution*: should coverage
 826 be with respect to $P_{X|T=1}$ (treated), $P_{X|T=0}$ (untreated), or a mixture P_X ? This point is empha-
 827 sized in Lei & Candès (2021). If one could attain conditional coverage, covariate shift would not
 828 pose a problem (recall that conditional coverage implies marginal coverage under any P_X) but such
 829 guarantees remain scarce (Gibbs et al., 2025).

830 To address distributional shift, weighted conformal prediction adjusts calibration via importance
 831 weights derived from the likelihood ratio between covariate distributions; when this ratio is known,
 832 one can guarantee exact marginal coverage for the chosen target population (Tibshirani et al., 2019).
 833 When the ratio (or propensity score $\pi(x)$) is estimated, asymptotically valid marginal coverage is
 834 still achievable, with strong empirical performance (Lei & Candès, 2021). Recent approaches re-
 835 fine this idea by incorporating likelihood-ratio regularization for high-dimensional covariates (Joshi
 836 et al., 2025) or leveraging unlabeled test data to adapt coverage under label scarcity (Kasa et al.,
 837 2025). For settings with both covariate shift and posterior drift, weighted conformal classifiers have
 838 been proposed (Wang & Qiao, 2025).

839
 840
 841
 842
 843
 844
 845
 846
 847
 848
 849
 850
 851
 852
 853
 854
 855
 856
 857
 858
 859
 860
 861
 862
 863

864 **B ADDITIONAL EXPERIMENTS: MISSPECIFIED ρ AND NON-GAUSSIANITY**
865866 **B.1 HOW VITAL IS THE ASSUMPTION OF GAUSSIANITY?**
867

868 We evaluate the sensitivity of our counterfactual estimation method to violations of the Gaussianity
869 assumption in the joint distribution of potential outcomes. Specifically, we use the Synthetic dataset
870 described in Appendix C.2, but replace the Gaussian error terms with non-Gaussian marginals cou-
871 pled through different copulas. Formally, for each unit i , we generate

$$872 \quad (\varepsilon_i^0, \varepsilon_i^1) \stackrel{i.i.d.}{\sim} \text{Copula}_\rho(F_0, F_1),$$

873 where F_t denotes the marginal distribution of ε_i^t (e.g., $t = 0, 1$ could follow Student- t , Laplace,
874 or Chi-square distributions), and Copula_ρ is a copula with correlation ρ . By Sklar's theorem, this
875 ensures that the joint distribution of $(\varepsilon_i^0, \varepsilon_i^1)$ has the specified marginals while preserving the de-
876 sired correlation structure through Copula_ρ . We experiment with Gaussian and Gumbel copulas to
877 capture symmetric as well as asymmetric dependence patterns.

878 We vary the following factors:
879

- 880 • Marginal distributions: Gaussian, Student- t ($df = 3$), Laplace, and Chi-square ($df = 3$),
- 881 • Copula families: Gaussian and Gumbel,
- 882 • Cross-world correlation: $\rho \in \{0, 0.5, 1\}$,
- 883 • Sample size: $n \in \{100, 300, 500, 2000\}$ with covariate dimension fixed at $d = 1$.

884 For each configuration, we generate 50 replications and compare our estimate $\hat{\mu}_\rho$ against the oracle
885 estimator

$$886 \quad \hat{Y}_{\text{oracle}}^{\text{cf}} := \mathbb{E}[Y^{\text{cf}} \mid X, Y^{\text{obs}}, T],$$

887 which leverages the true joint distribution. We report the performance gap
888

$$889 \quad \text{Gap} = \text{MSE}_{\text{our}} - \text{MSE}_{\text{oracle}}, \quad \text{MSE}_{\text{our}} = \frac{1}{n} \sum_{i=1}^n (\hat{Y}_i^{\text{cf}} - Y_i^{\text{cf}})^2, \quad \hat{Y}_i^{\text{cf}} = \hat{\mu}_\rho.$$

890 Figure 4 summarizes the results. In all cases, the gap decreases with n , demonstrating that our
891 estimator converges to the oracle regardless of the marginal distribution or copula. The effect
892 of non-Gaussianity is therefore limited to finite samples: convergence is noticeably slower under
893 heavy-tailed or skewed marginals, particularly when $\rho = 1$, but the asymptotic behavior remains
894 unchanged. By contrast, under independence ($\rho = 0$), our estimator is nearly indistinguishable from
895 the oracle even in small samples.

896 **In conclusion, violations of Gaussianity do not seem to threaten the validity of our method, but
897 they can slow finite-sample convergence; especially under large cross-world dependence.**

900 **B.2 DETAILS ABOUT FIGURE 3 AND MISSPECIFIED ρ**

901 To study the effect of misspecifying the cross-world correlation ρ , we carried out a grid experiment
902 on synthetic data. For each design point, we distinguish between the **true** value ρ_{true} used in the
903 data-generating process (DGP), and the **assumed** value ρ_{est} used in our estimator $\hat{\mu}_\rho$.

904 We consider the *synthetic* dataset (see Section C.1), a univariate covariate setting ($d = 1$), two
905 sample sizes ($n = 200$ and $n = 2000$), and repeated each experiment 50 times to reduce Monte
906 Carlo variability. The true correlation ρ_{dgp} was varied over a grid $\{0, 0.1, \dots, 1\}$, and for each value
907 we estimated counterfactuals under a grid of assumed correlations $\rho_{\text{est}} \in \{0, 0.1, \dots, 1\}$.

908 For each pair $(\rho_{\text{true}}, \rho_{\text{est}})$, we generated synthetic data, computed counterfactual estimates with our
909 method using ρ_{est} , and compared performance against the oracle estimator $\mathbb{E}[Y^{\text{cf}} \mid X, Y^{\text{obs}}, T]$. We
910 measured performance using the mean squared error (MSE) of counterfactual predictions, and sum-
911 marized results via the $\text{Gap} = \text{MSE}_{\text{our}} - \text{MSE}_{\text{oracle}}$. Results (Figure 3) show that the gap increases
912 systematically with the degree of misspecification $|\rho_{\text{est}} - \rho_{\text{true}}|$. When the assumed correlation is
913 close to the truth, the gap shrinks as n grows, and bias vanishes asymptotically. In contrast, for

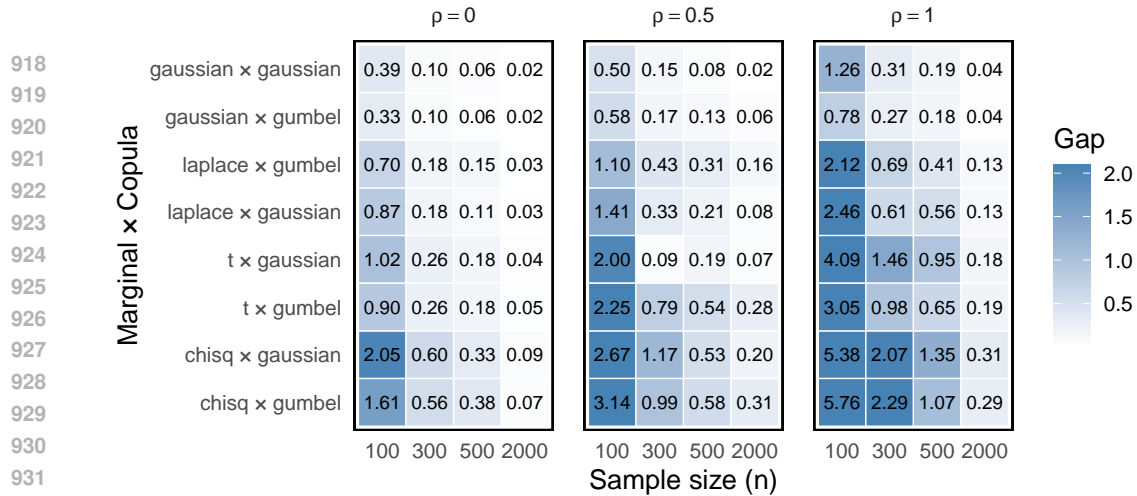


Figure 4: $\text{Gap} = \text{MSE}_{\text{our}} - \text{MSE}_{\text{oracle}}$ calculated across different marginal-copula distributions of potential outcomes $(Y(0), Y(1))$. Here, we only considered correctly specified ρ in the estimation.

larger misspecifications, the bias persists even at large n , indicating that asymptotic consistency requires $\rho_{\text{est}} \approx \rho_{\text{true}}$. These results show the importance of approximate domain knowledge of ρ : even approximate information about its value can yield large gains over methods that implicitly assume $\rho = 0$ or $\rho = 1$.

941
942
943
944
945
946
947
948
949
950
951
952
953
954
955
956
957
958
959
960
961
962
963
964
965
966
967
968
969
970
971

972 C APPENDIX: NUMERICAL EXPERIMENTS
973974 We provide full details about our experiments below.
975976 C.1 DATASETS
977978 We investigate three types of data-generating mechanisms:
979

- **Synthetic** (taken from (Bodik et al., 2025)): For the univariate case ($d = 1$), we draw $X \sim \text{Unif}(-1, 1)$. When $d > 1$, we follow the setup in Wager & Athey (2018); Alaa et al. (2023); Lei & Candès (2021); Jonkers et al. (2024) and generate covariates $\mathbf{X} = (X_1, \dots, X_d)$, where each $X_j = \Phi(\tilde{X}_j)$ and Φ is the standard normal CDF. The latent vector $(\tilde{X}_1, \dots, \tilde{X}_d)$ is sampled from a multivariate Gaussian distribution with zero mean and constant pairwise correlation $\text{Cov}(\tilde{X}_j, \tilde{X}_{j'}) = 0.25$ for $j \neq j'$. Treatment assignments are drawn from a propensity score function

$$\pi(\mathbf{X}) = \frac{1 + |X_1|}{4} \in [0.25, 0.5],$$

990 ensuring adequate overlap. The potential outcomes are defined as

$$\begin{aligned} Y_i(0) &= f_0(\mathbf{X}_i) + \varepsilon_i^0, \\ Y_i(1) &= f_0(\mathbf{X}_i) + \tau(\mathbf{X}_i) + \varepsilon_i^1, \end{aligned}$$

994 with noise terms jointly distributed as

$$(\varepsilon_i^0, \varepsilon_i^1) \sim \mathcal{N}\left(\begin{bmatrix} 0 \\ 0 \end{bmatrix}, \begin{bmatrix} 1 & 2\rho \\ 2\rho & 4 \end{bmatrix}\right).$$

998 The treatment effect function $\tau(\mathbf{x}) = \tau(x_1, x_2)$ is a smooth random polynomial depending
999 on the first two covariates (or only on x_1 when $d = 1$), generated using a Perlin noise generator
1000 (Perlin, 1985) following Bodik & Chavez-Demoulin (2025). The baseline function
1001 is $f_0(x) = \beta^\top x$ with β drawn from a standard normal distribution.

- **IHDP (semi-synthetic):** Originally introduced in Hill (2011), this dataset contains 25 pre-treatment covariates (e.g., birth weight, maternal age, education level) denoted by \mathbf{X} . The binary treatment T indicates whether the infant participated in the intervention program. Potential outcomes represent cognitive test scores, were simulated in Hill (2011) as

$$Y_i(0) = f_0(X_i) + \varepsilon_i^0, \tag{6}$$

$$Y_i(1) = f_1(X_i) + \varepsilon_i^1, \tag{7}$$

1010 where $\varepsilon_i^0, \varepsilon_i^1 \stackrel{\text{i.i.d.}}{\sim} N(0, 1)$. The functions f_0 and f_1 are either random linear (case “A”) or
1011 nonlinear (case “B”). We only consider case “B”.

1012 While the original setup fixes $\rho = 0$, we also consider a correlated noise version:

$$\begin{pmatrix} \varepsilon_i^0 \\ \varepsilon_i^1 \end{pmatrix} \stackrel{\text{i.i.d.}}{\sim} \mathcal{N}\left(\begin{pmatrix} 0 \\ 0 \end{pmatrix}, \begin{pmatrix} 1 & \rho \\ \rho & 1 \end{pmatrix}\right).$$

1016 which better reflects empirical situations in which the two potential outcomes are not independent
1017 but share substantial underlying information.

- **Twins (real-world):** We use the U.S. twin birth records (1989–1991) described in Louizos et al. (2017), restricted to same-sex twins with both birth weights below 2 kg. Each pair comes with detailed perinatal covariates, including maternal risk factors, prenatal care indicators, and demographic information. In this context, twins are viewed as natural counterfactuals for one another, so the potential outcomes can be conceptually “observed” by comparing mortality for the heavier twin ($T = 1$) and the lighter twin ($T = 0$) within the same pair. The outcome variable is one-year mortality. In our analysis, we work with a balanced sample containing a moderate number of individuals and a small set of covariates, obtained after standard preprocessing.

1026
1027C.2 INTERVAL SCORES RESULTS: USE C_ρ FOR $\rho \leq 0.5$ AND C_ρ^{+CI} FOR $\rho > 0.5$ 1028
1029
1030
1031
1032
1033
1034
1035

Figures 5 and 6 report the Interval Scores (IS) of the competing methods across all datasets considered in our experiments. The Interval Score jointly evaluates interval width and coverage, with lower values indicating more efficient and reliable prediction intervals. While GANITE is excluded from these comparisons because it does not provide prediction intervals out of the box, one could imagine extending it with Bayesian or conformalized post-processing layers to quantify uncertainty. For instance, sampling-based approaches could be added to its adversarial generator, or conformal calibration could be applied on top of GANITE outputs. However, such adaptations are not standard, and we therefore omit GANITE from the interval score plots.

1036
1037
1038
1039
1040
1041
1042
1043
1044
1045

Results. When using the bias-corrected C_ρ^{+CI} variant, our method achieves consistently strong results, typically outperforming all baselines across datasets. The only exception is when $\rho = 0$, in which case Direct Outcome (DO) estimators attain nearly identical performance. The main drawback of C_ρ^{+CI} lies in its computational cost, since constructing bootstrap confidence intervals is substantially more demanding than computing C_ρ . Moreover, when ρ is large, estimation error in $\hat{\mu}_\rho$ can induce bias, leading to undercoverage and consequently poor Interval Scores. In practice, we therefore recommend using the uncorrected C_ρ intervals when $\rho \leq 0.5$, while for $\rho > 0.5$ the bias-corrected C_ρ^{+CI} intervals are preferable, as they yield the greatest empirical gains.

Recommendation: C_ρ is satisfactory if $\rho \leq 0.5$, and ideally use C_ρ^{+CI} if $\rho > 0.5$.

1046
1047
1048
1049
1050
1051
1052
1053
1054
1055
1056
1057
1058
1059
1060
1061
1062
1063
1064
1065
1066
1067
1068
1069
1070
1071
1072
1073
1074
1075
1076
1077
1078
1079

Interval Scores of different prediction intervals (Ranked)												
Synthetic						Real data						
1080	d= 1, p = 0.00	5.77 / 5.91	5.81	13.27	10.21	NaN	IHDP d= 1, p = 0.00	8.02 / 7.85	8.15	48.14	13.69	NaN
1081	d= 1, p = 0.25	5.63 / 5.88	5.84	11.67	10.26	NaN	IHDP d= 1, p = 0.25	7.73 / 7.90	8.28	43.84	13.99	NaN
1082	d= 1, p = 0.50	5.10 / 5.57	5.86	10.03	10.24	NaN	IHDP d= 1, p = 0.50	8.56 / 9.24	9.42	55.64	15.50	NaN
1083	d= 1, p = 0.75	4.04 / 5.61	5.83	8.72	10.15	NaN	IHDP d= 1, p = 0.75	6.95 / 9.85	7.70	37.03	12.85	NaN
1084	d= 10, p = 0.00	6.92 / 6.94	6.98	9.03	11.79	NaN	IHDP d= 10, p = 0.00	13.10 / 9.48	7.27	34.58	12.07	NaN
1085	d= 10, p = 0.25	6.81 / 6.86	7.04	8.37	11.77	NaN	IHDP d= 10, p = 0.25	6.10 / 6.05	6.33	10.17	9.98	NaN
1086	d= 10, p = 0.50	6.35 / 6.52	7.00	7.71	11.68	NaN	IHDP d= 10, p = 0.50	5.55 / 5.65	6.26	8.58	9.63	NaN
1087	d= 10, p = 0.75	5.62 / 6.17	6.99	7.13	11.75	NaN	IHDP d= 10, p = 0.75	5.42 / 6.08	6.58	9.06	10.17	NaN
1088	d= 10, p = 1.00	5.12 / 5.19	7.02	6.84	11.81	NaN	IHDP d= 10, p = 1.00	6.84 / 6.25	6.67	9.23	10.20	NaN
1089	C _p ^{+CI}	DO	cate-adj	matching	ganite		C _p ^{+CI}	DO	cate-adj	matching	ganite	
1090	$\rho_{\text{correct}} / \rho_{\text{misspec}}$	(CQR)	(<i>T</i> -learner)	(Mah. dist.)			$\rho_{\text{correct}} / \rho_{\text{misspec}}$	(CQR)	(<i>T</i> -learner)	(Mah. dist.)		
1091	Rank (IS)  1 (best) 2 3 4 (Missing)											
1092												
1093												
1094												
1095												
1096												
1097												
1098												
1099												
1100												
1101												
1102	Figure 5: Interval Scores of different prediction interval methods across all datasets. Here, C_p^{+CI} , the bias-corrected version of C_p introduced in Section 3.3, is used. GANITE is excluded since it does not provide a natural way of constructing prediction intervals.											
1103												
1104												
1105												
1106												
1107												
1108												
1109	Synthetic						Real data					
1110	d= 1, p = 0.00	5.79	5.94	5.81	13.26	10.21	IHDP d= 1, p = 0.00	8.05	7.96	8.15	47.97	13.69
1111	d= 1, p = 0.25	5.64	5.94	5.84	11.66	10.26	IHDP d= 1, p = 0.25	7.77	7.96	8.28	43.72	13.99
1112	d= 1, p = 0.50	5.11	6.16	5.86	10.06	10.24	IHDP d= 1, p = 0.50	12.36	10.04	9.42	55.75	15.50
1113	d= 1, p = 0.75	4.04	7.36	5.83	8.71	10.15	IHDP d= 1, p = 0.75	65.07	13.70	7.70	37.17	12.85
1114	d= 10, p = 0.00	6.95	7.00	6.98	9.04	11.79	IHDP d= 10, p = 0.00	55.13	14.12	7.27	34.48	12.07
1115	d= 10, p = 0.25	6.84	7.20	7.02	8.37	11.77	IHDP d= 10, p = 0.25	6.17	6.12	6.36	10.22	9.98
1116	d= 10, p = 0.50	6.40	8.27	7.00	7.71	11.68	IHDP d= 10, p = 0.50	6.68	6.88	7.11	12.18	11.09
1117	d= 10, p = 0.75	5.75	8.91	6.98	7.13	11.75	IHDP d= 10, p = 0.75	5.67	6.72	6.25	8.60	9.63
1118	d= 10, p = 1.00	5.56	11.97	7.02	6.85	11.81	IHDP d= 10, p = 1.00	7.32	11.52	6.72	9.22	10.20
1119	C _p	C _p	DO	cate-adj	matching		C _p	C _p	DO	cate-adj	matching	
1120	ρ_{correct}	ρ_{misspec}	(CQR)	(<i>T</i> -learner)	(Mah. dist.)		ρ_{correct}	ρ_{misspec}	(CQR)	(<i>T</i> -learner)	(Mah. dist.)	
1121												
1122												
1123												
1124												
1125												
1126												
1127	Rank (IS, lower = better)  1 (best) 2 3 4 5 (worst)											
1128												
1129												
1130												
1131												
1132	Figure 6: Interval Scores of different prediction interval methods across all datasets. Here, the uncorrected C_p intervals, as defined in Section 3, are used.											
1133												



Figure 7: Extended version of Figure 2, additionally displaying the standard deviations of the MSE estimates within each cell.

1188 **D PROOFS**
 1189

1190 **Theorem 1** (Motivation and optimality under a perfect (asymptotic) scenario). *Let $x \in \mathcal{X}$, and*
 1191 *$\rho = \text{cor}(Y(0), Y(1) | X = x) \in [-1, 1]$. Assume a perfect scenario: $(Y(1), Y(0)) | X = x$ is*
 1192 *Gaussian, $\hat{\mu}_t(x) = \mu_t(x)$ and suppose that we found conditionally valid prediction intervals:*

1193 $\mathbb{P}(Y(t) \leq \hat{\mu}_t(x) + u_t(x) | X = x) = 0.95, \quad \mathbb{P}(Y(t) \geq \hat{\mu}_t(x) - l_t(x) | X = x) = 0.95, \quad t = 0, 1.$

1194 Then, C_ρ prediction intervals from Definition 2 are optimal in a sense that it is the smallest set
 1195 satisfying:

1196
$$\mathbb{P}(Y(1) \in C_\rho(X, Y(0)) | X = x, Y(0) = y) \geq 0.9,$$

1197 for any $y \in \mathbb{R}$. Moreover, $\hat{\mu}_\rho(x, y)$ is the optimal point predictor in the sense that it minimizes the
 1198 mean squared error:

1199
$$\hat{\mu}_\rho(x, y) = \underset{c \in \mathbb{R}}{\text{argmin}} \mathbb{E}[(Y(1) - c)^2 | X = x, Y(0) = y].$$

1200 *Proof.* We use the following fact:

1201 For a bivariate Gaussian random variables (Z_1, Z_0) :

1202
$$\begin{pmatrix} Z_0 \\ Z_1 \end{pmatrix} \sim \mathcal{N} \left(\begin{pmatrix} \mu_0 \\ \mu_1 \end{pmatrix}, \begin{pmatrix} \sigma_0^2 & \rho\sigma_0\sigma_1 \\ \rho\sigma_0\sigma_1 & \sigma_1^2 \end{pmatrix} \right),$$

1203 it is well known that:

1204
$$Z_1 | Z_0 = z \sim \mathcal{N} \left(\mu_1 + \rho \frac{\sigma_1}{\sigma_0} (z - \mu_0), \sigma_1^2 (1 - \rho^2) \right).$$

1205 Moreover, the shortest prediction interval with a given coverage is symmetric around the mean.

1206 First, we introduce some notation:

- 1207 • Let $c := \Phi^{-1}(0.95) \approx 1.6449$ denote the 0.95 quantile of a standard Gaussian random
 1208 variable.
- 1209 • Let $\sigma_t^2(x) := \text{Var}(Y(t) | X = x)$ denote the conditional variance.
- 1210 • $\mu_t(x) + u_t(x) = \text{Quantile}_{0.95}(Y(t) | X = x)$.
- 1211 • Since $Y(t) | X = x$ is symmetrical around the mean, we have $l_t(x) = u_t(x)$. Therefore,
 1212 $u_t(x) = c \cdot \sigma_t(x)$, by the standard form of the quantile function for a Gaussian distribution.
 1213 Therefore, $\lambda(x) = \frac{\sigma_1(x)}{\sigma_0(x)}$.

1214 Due to Gaussianity assumption, it holds that:

1215
$$Y(1) | Y(0) = y, X = x \sim \mathcal{N} \left(\mu_1(x) + \rho \frac{\sigma_1(x)}{\sigma_0(x)} (y - \mu_0(x)), (1 - \rho^2) \sigma_1^2(x) \right)$$

1216 which directly gives us

1217
$$\mathbb{P}(Y(1) \leq \mu_1(x) + \rho \frac{\sigma_1(x)}{\sigma_0(x)} (y_0 - \mu_0(x)) + \sqrt{1 - \rho^2} \cdot c \cdot \sigma_1(x) | X = x, Y(0) = y_0) = 0.95.$$

1218 Using our notation and previously established results, we get

1219
$$\mathbb{P}(Y(1) \leq \hat{\mu}_\rho(x, y_0) + \sqrt{1 - \rho^2} \cdot u_1(x) | X = x, Y(0) = y_0) = 0.95,$$

1220 and analogously

1221
$$\mathbb{P}(Y(1) \geq \hat{\mu}_\rho(x, y_0) - \sqrt{1 - \rho^2} \cdot l_1(x) | X = x, Y(0) = y_0) = 0.95.$$

1242 Hence, we proved that

$$1243 \quad \mathbb{P}(Y(1) \in C_\rho(X, Y(0)) \mid X = x, Y(0) = y_0) = 0.9.$$

1244 The fact that C_ρ prediction interval is the smallest possible interval achieving the desired coverage
1245 follows directly from symmetry+continuity of Gaussian variable.

1246 The fact that $\hat{\mu}_\rho(x, y)$ is the optimal point predictor follows directly since

$$1247 \quad \hat{\mu}_\rho(x, y) = \mathbb{E}[Y(1) \mid X = x, Y(0) = y].$$

1248 \square

1249 **Theorem 2.** Let $x \in \mathcal{X}$ and suppose $(Y(1), Y(0)) \mid X = x$ is Gaussian with $\rho = \text{cor}(Y(1), Y(0) \mid$
1250 $X = x) \in [-1, 1]$.

1251 Let $\hat{\mu}_t(x)$ be consistent estimators of $\mu_t(x)$, and assume the prediction interval widths $l_t(x), u_t(x)$
1252 are asymptotically conditionally valid, i.e.,

$$1253 \quad \lim_{n \rightarrow \infty} \mathbb{P}(Y(t) \leq \hat{\mu}_t(x) + u_t(x) \mid X = x) = 0.95, \quad \lim_{n \rightarrow \infty} \mathbb{P}(Y(t) \geq \hat{\mu}_t(x) - l_t(x) \mid X = x) = 0.95,$$

1254 for $t = 0, 1$. Then, for any fixed $y \in \mathbb{R}$:

1255 1. $\hat{\mu}_\rho(x, y)$ is a consistent estimator of the conditional mean,

$$1256 \quad \hat{\mu}_\rho(x, y) \xrightarrow{p} \mathbb{E}[Y(1) \mid X = x, Y(0) = y], \quad \text{as } n \rightarrow \infty.$$

1257 2. The C_ρ prediction intervals achieve asymptotic conditional coverage,

$$1258 \quad \lim_{n \rightarrow \infty} \mathbb{P}(Y(1) \in C_\rho(X, Y(0)) \mid X = x, Y(0) = y) = 0.9.$$

1259 *Proof.* Under the Gaussian assumption, Theorem 1 implies

$$1260 \quad \mathbb{E}[Y(1) \mid X = x, Y(0) = y] = \mu_1(x) + \rho \frac{\sigma_1(x)}{\sigma_0(x)} (y - \mu_0(x)). \quad (8)$$

1261 By consistency, $\hat{\mu}_t(x) \xrightarrow{p} \mu_t(x)$ for $t = 0, 1$. Moreover, since the upper and lower bounds converge
1262 to the 0.95 and 0.05 conditional quantiles of $Y(t) \mid X = x$, their total width satisfies

$$1263 \quad l_t(x) + u_t(x) \xrightarrow{p} \text{Quantile}_{0.95}(Y(t) \mid X = x) - \text{Quantile}_{0.05}(Y(t) \mid X = x) = 2z_{0.95}\sigma_t(x).$$

1264 Thus,

$$1265 \quad \lambda(x) = \frac{l_1(x) + u_1(x)}{l_0(x) + u_0(x)} \xrightarrow{p} \frac{\sigma_1(x)}{\sigma_0(x)}.$$

1266 Substituting into $\hat{\mu}_\rho(x, y)$,

$$1267 \quad \hat{\mu}_\rho(x, y) \xrightarrow{p} \mu_1(x) + \rho \frac{\sigma_1(x)}{\sigma_0(x)} (y - \mu_0(x)),$$

1268 which coincides with equation 8, proving consistency of the point estimator.

1269 For the prediction interval C_ρ , Theorem 1 further states that, under Gaussianity, $C_\rho(X, Y(0))$ is the
1270 minimal set achieving 90% conditional coverage for $Y(1) \mid X = x, Y(0) = y$. Since $l_t(x)$ and
1271 $u_t(x)$ converge to their true quantiles, the constructed interval converges to this optimal set. Hence,

$$1272 \quad \lim_{n \rightarrow \infty} \mathbb{P}(Y(1) \in C_\rho(X, Y(0)) \mid X = x, Y(0) = y) = 0.9.$$

1273 \square

1274 **Lemma 1** (Special cases of ρ). • If $\rho = 0$ and $\tilde{C}_1(X)$ is marginally valid, then $C_\rho(X, Y(0))$
1275 is also marginally valid:

$$1276 \quad \mathbb{P}(Y(1) \in \tilde{C}_1(X)) \geq 0.9 \implies \mathbb{P}(Y(1) \in C_\rho(X, Y(0))) \geq 0.9.$$

1277 If additionally $Y(0) \perp\!\!\!\perp Y(1) \mid X = x$ and $\tilde{C}_1(X)$ is conditionally valid, then
1278 $C_\rho(X, Y(0))$ is also conditionally valid:

$$1279 \quad \mathbb{P}(Y(1) \in \tilde{C}_1(X) \mid X = x) \geq 0.9 \implies \mathbb{P}(Y(1) \in C_\rho(X, Y(0)) \mid X = x, Y(0) = y) \geq 0.9,$$

1280 for any $x \in \mathcal{X}, y \in \mathcal{Y}$.

1296 • If $\rho = \pm 1$ and $\mu(x, y_0) = \hat{\mu}(x, y_0)$, then
 1297

$$1298 \quad \mathbb{P}(Y(1) \in C_\rho(X, Y(0)) \mid X = x, Y(0) = y) = 1.$$

1299 If we have confidence intervals satisfying $\mathbb{P}(\mu(x, y_0) \in \hat{\mu}(x, y_0) \pm r(x, y_0)) = 1 - \beta$, then
 1300

$$1301 \quad \mathbb{P}(Y(1) \in C_\rho^{+CI}(X, Y(0)) \mid X = x, Y(0) = y) = 1 - \beta.$$

1302
 1303 *Proof.* **Case $\rho = 0$:** By definition, $C_\rho(X, Y(0)) = \tilde{C}_1(X)$, so marginal validity is preserved. If
 1304 $Y(0) \perp\!\!\!\perp Y(1) \mid X$, then conditioning on $Y(0)$ does not affect the validity, hence conditional validity
 1305 also holds.

1306 **Case $\rho = \pm 1$:** Perfect (anti-)correlation implies a deterministic linear relationship: for fixed $X = x$,
 1307 we have

$$1308 \quad Y(1) = a_x + b_x Y(0) \quad \text{for some } a_x, b_x \in \mathbb{R}.$$

1309 Thus,

$$1311 \quad \text{Var}(Y(1) \mid X = x, Y(0) = y) = 0 \quad \Rightarrow \quad \mathbb{P}(Y(1) = \mu(x, y) \mid X = x, Y(0) = y) = 1.$$

1312 If $\mu(x, y) = \hat{\mu}(x, y)$, then $C_\rho(x, y) = \{\mu(x, y)\}$, implying perfect coverage. If instead $\mu(x, y)$ lies
 1313 in a confidence interval with coverage $1 - \beta$, then
 1314

$$1315 \quad \mathbb{P}(Y(1) \in C_\rho^{+CI}(x, y) \mid X = x, Y(0) = y) \geq 1 - \beta.$$

1316 □

1317
 1318
 1319
 1320
 1321
 1322
 1323
 1324
 1325
 1326
 1327
 1328
 1329
 1330
 1331
 1332
 1333
 1334
 1335
 1336
 1337
 1338
 1339
 1340
 1341
 1342
 1343
 1344
 1345
 1346
 1347
 1348
 1349